

Increase and Limit of $T_{\theta 2}$ in Super- and Hypersonic Flight

Gottfried Sachs*
Technical University of Munich,
D-85747 Munich, Germany

Introduction

A PRIMARY flying qualities metric is the numerator zero $1/T_{\theta 2}$ of the pitch attitude to pitch control transfer function.¹⁻⁴ It describes the lag between the responses of the pitch attitude and the flight path to a pitch control input. A well-balanced relation in the time responses, qualified as path-attitude consonance, is of paramount significance for longitudinal control.

The extension of the speed regime to super- and hypersonic flight is associated with a substantial increase of $T_{\theta 2}$, leading to values of 25 s or more. The resulting flying qualities problems are an issue of continuous interest, and there is a controversial discussion concerning the reasons for the increase of $T_{\theta 2}$ (Refs. 3-9). In several discussions, the lift curve slope $C_{L\alpha}$ plays an important role.⁴⁻⁶ In particular, the $T_{\theta 2}$ increase is considered to be due to the very low $C_{L\alpha}$ of hypersonic vehicles because of their unique aerodynamic configuration. Other investigations indicate that there are further reasons for the addressed path-attitude control problem.^{8,9} This concerns a low-frequency washout characteristic in the flight-path response due to altitude effects.

It is the purpose of this Note to suggest a mechanism causing the addressed increase of $T_{\theta 2}$. It will be shown that the $C_{L\alpha}$ effect may not be considered separately but as a part of an overall aerodynamic effect, which does not change much, even when comparing the conventional and the hypersonic regions. Further, the speed and the atmospheric density gradient are identified as main factors for the increase of $T_{\theta 2}$.

A further purpose of this Note is to show that there is a limiting effect caused by the atmospheric density gradient, yielding an upper bound on $T_{\theta 2}$. It turns out that this limit is practically independent of speed or Mach number, respectively.

Aerodynamics and Speed Effects on $T_{\theta 2}$ Increase

The aircraft dynamics of concern for the problems in mind are usually described by the short-term pitch model yielding the following transfer function:

$$\frac{\theta(s)}{\delta_e(s)} = \frac{M_\delta(s + 1/T_{\theta 2})}{s(s^2 + 2\zeta_{sp}\omega_{sp}s + \omega_{sp}^2)} \quad (1)$$

The numerator consists of a first-order zero ($-1/T_{\theta 2}$) and the denominator yields second-order poles representing the short-period mode of motion (ω_{sp} , ζ_{sp}). This model can be used for unaugmented aircraft as well as for augmented vehicles with the addition of a time delay $e^{-\tau s}$ in the numerator when applying the lower-order equivalent system concept.¹

The numerator zero may be described by the following expression:

$$T_{\theta 2} \approx (V_0/g)C_L/C_{L\alpha} \quad (2)$$

Thus, the aerodynamic influence is due to C_L and $C_{L\alpha}$: $T_{\theta 2} \propto C_L/C_{L\alpha}$.

Super- and hypersonic vehicles have very low $C_{L\alpha}$ because of their unique aerodynamic configuration. This characteristic is presented in Fig. 1a, which also shows that increasing Mach number leads

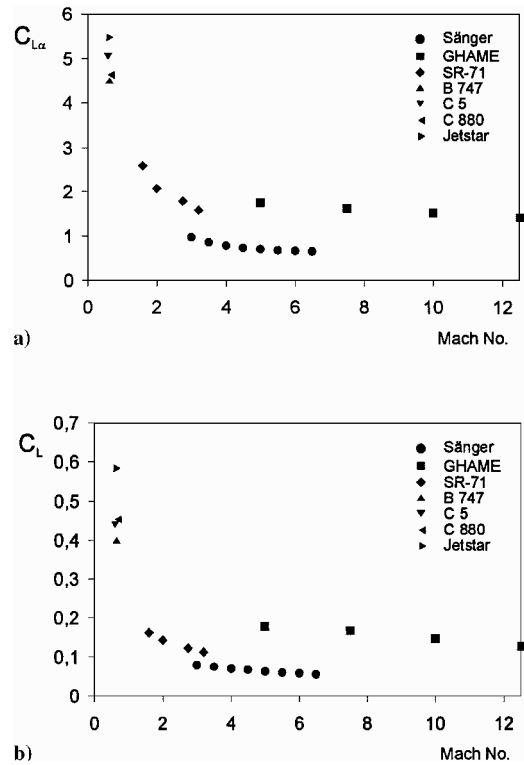


Fig. 1 Lift curve slope and lift coefficient (maximum lift-to-drag ratio), data from Refs. 10-13.

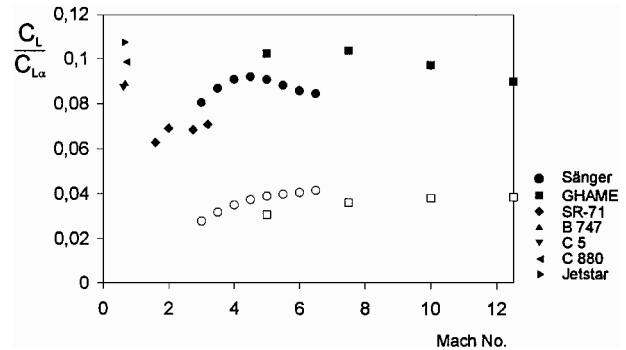


Fig. 2 Overall aerodynamics effect $C_L/C_{L\alpha}$, data from Refs. 10-13: filled symbols, maximum lift-to-drag ratio; and open symbols, high dynamic pressure flight ($\bar{q}_{\max} = 50$ kPa).

to a further decrease. Comparison with conventional-speed aircraft reveals that there is a significant decrease of $C_{L\alpha}$ for super- and hypersonic vehicles. The results presented in Fig. 1, with data from Refs. 10-13, suggest that the reduction in $C_{L\alpha}$ is the main reason for the increase of $T_{\theta 2}$.

However, typical configurations of super- and hypersonic vehicles are also associated with reduced C_L values that may be aerodynamically feasible or utilizable for the flight tasks and operations of these vehicles. This feature is depicted in Fig. 1b, which shows that super- and hypersonic vehicles have low C_L values, particularly when compared with aircraft of the conventional-speed region.

As a result, the C_L reduction due to the aerodynamic configuration of hypersonic vehicles basically shows a similarity to the $C_{L\alpha}$ decrease. From these properties, both caused by the unique configuration of hypersonic vehicles, it follows that the $C_{L\alpha}$ effect may not be considered separately but as part of an overall aerodynamics effect set by the ratio $C_L/C_{L\alpha}$. This interpretation is illustrated in Fig. 2, which shows two $C_L/C_{L\alpha}$ curves for representative flight tasks: One curve relates to the maximum aerodynamic performance (maximum lift-to-drag ratio), which is of particular concern for cruise type vehicles. The other curve corresponds to high dynamic pressure flight, which may be of interest for hypersonic acceleration type vehicles. Figure 2 reveals that the $C_L/C_{L\alpha}$ ratio shows only little change,

Received Sept. 19, 1997; revision received June 1, 1998; accepted for publication June 29, 1998. Copyright © 1998 by Gottfried Sachs. Published by the American Institute of Aeronautics and Astronautics, Inc., with permission.

*Professor, Institute of Flight Mechanics and Flight Control. Fellow AIAA.

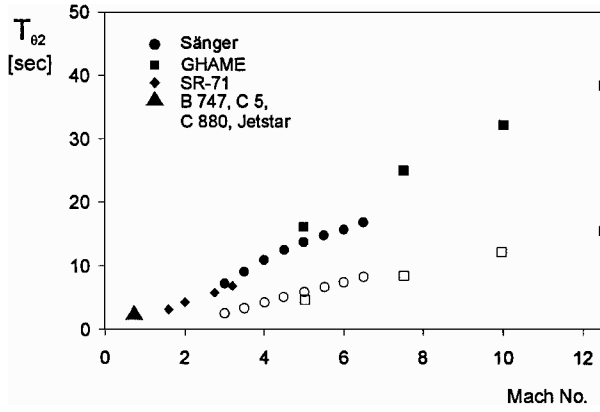


Fig. 3 Increase of $T_{\theta 2}$ according to constant atmospheric density modeling Eq. (2), data from Refs. 10–13: filled symbols, maximum lift-to-drag ratio; and open symbols, high dynamic pressure flight ($\bar{q}_{\max} = 50$ kPa).

staying at rather constant level. This feature even applies when comparing vehicles of the conventional-speed region and the hypersonic regime.

An evaluation of the $T_{\theta 2}$ characteristics of the configurations just considered is shown in Fig. 3. There are several observations to be made from Fig. 3 concerning the features of the $T_{\theta 2}$. Basically, $T_{\theta 2}$ steadily increases with Mach number (or speed, respectively), and there seems to be no limit. The increase of $T_{\theta 2}$ approximately follows a straight line suggesting a proportionality to Mach number or speed, respectively. Based on this characteristic and on the interpretation of the aerodynamics effects considered in the preceding paragraphs, it may be concluded that speed is the primary factor for the increase of $T_{\theta 2}$.

$T_{\theta 2}$ Limit and Increase Due to Atmospheric Density Gradient

The analysis concerning the $T_{\theta 2}$ characteristics shown in Fig. 3 is based on the short-term dynamics model Eq. (1), which assumes constant atmospheric density. For super- and hypersonic flight, an extension of the aircraft dynamics model is necessary to account for the effect of the atmospheric density gradient on $T_{\theta 2}$. This effect primarily leads to an upper limit beyond which no $T_{\theta 2}$ values are possible.

From an aircraft dynamics model accounting for the change of atmospheric density with altitude,¹⁴ it follows that the numerator of the pitch attitude to pitch control function is of second order, instead of first order as in Eq. (1), for the frequency range under consideration

$$N_{\delta}^{\theta}(s) = M_{\delta} [s^2 + s(g/V_0)C_{L\alpha}/C_L - g\rho_h] \quad (3)$$

Accordingly, there are two zeros. They are real valued in supersonic and low hypersonic flight. The larger one corresponds to $1/T_{\theta 2}$, and the smaller one, which may be denoted by $1/T_{\theta\rho}$, is due to the effect of the density gradient $\rho_h = (1/\rho) d\rho/dh$. From Eq. (3) it follows that an increase of speed causes the two zeros to move toward each other as regards their size until they become equal. Then, they couple into a complex pair. From Eq. (3), the condition for both zeros being equal ($1/T_{\theta 2} = 1/T_{\theta\rho}$) yields

$$T_{\theta 2} = (T_{\theta 2})_{\max} = \frac{1}{\sqrt{-g\rho_h}} \quad (4)$$

This is the largest value $T_{\theta 2}$ can attain. A larger value is basically not possible because of the addressed coupling of $T_{\theta 2}$ with $T_{\theta\rho}$ into a complex pair.

From Eq. (4) it follows that there is practically no effect of Mach number on $(T_{\theta 2})_{\max}$. Further, the altitude influence is rather small because the atmosphere shows only little changes of ρ_h for the whole altitude range that may be of interest for hypersonic flight.¹⁴ As a consequence, the limit $(T_{\theta 2})_{\max}$ is rather constant.

A numerical evaluation is presented in Fig. 4. As a main feature, the limit $(T_{\theta 2})_{\max}$ shows practically no dependency on Mach number

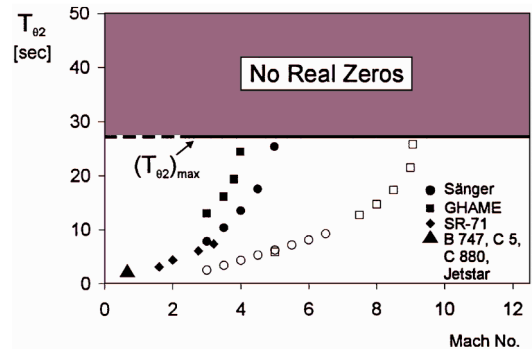


Fig. 4 Limit $(T_{\theta 2})_{\max}$ and more rapid increase of $T_{\theta 2}$, effects of atmospheric density gradient, data from Refs. 10–13: filled symbols, maximum lift-to-drag ratio; and open symbols, high dynamic pressure flight ($\bar{q}_{\max} = 50$ kPa).

or speed, respectively. Figure 4 further reveals that the $(T_{\theta 2})_{\max}$ limit is of the order of 25–30 s. The numerical value applied for ρ_h in the computations for Fig. 4 represents an average for the altitude range from 10 to 80 km. According to the atmospheric properties in this altitude range, there may be changes in $(T_{\theta 2})_{\max}$ up to $\pm 8\%$, depending on the actual ρ_h .

Note that the results for the limit of $T_{\theta 2}$ according to Eq. (4) and for its numerical value according to Fig. 4 are of general nature for super- and hypersonic flight.

Figure 4 further shows that the increase of $T_{\theta 2}$ with speed (or Mach number) is also influenced by the atmospheric density gradient. The increase of $T_{\theta 2}$ becomes much more rapid when the limit $(T_{\theta 2})_{\max}$ is approached. This outcome is in contrast to the results of the constant density model of Eq. (2), which shows no such change (Fig. 3). The effect of the atmospheric density gradient on the increase of $T_{\theta 2}$ is confirmed by the following expression:

$$T_{\theta 2} \approx \frac{2T_{\theta 2, \rho_h=0}}{1 + \sqrt{1 + 4g\rho_h T_{\theta 2, \rho_h=0}^2}} \quad (5)$$

where $T_{\theta 2, \rho_h=0} \approx (V_0/g)C_L/C_{L\alpha}$ denotes the constant density case Eq. (2).

Because of the more rapid $T_{\theta 2}$ increase caused by the atmospheric density gradient, the $(T_{\theta 2})_{\max}$ limit may be reached at rather low Mach numbers. Figure 4 also shows this effect according to which the $(T_{\theta 2})_{\max}$ limit can be reached at Mach numbers as low as $M = 4.0$ for flight conditions at maximum lift-to-drag ratio. For smaller lift coefficients, as in high dynamic pressure flight, the $(T_{\theta 2})_{\max}$ limit is approached at higher Mach numbers.

Conclusions

The numerator zero of the pitch attitude to pitch control transfer function ($-1/T_{\theta 2}$) is considered with regard to its characteristics in supersonic and hypersonic flight. It is shown that speed is a primary factor for the increase of $T_{\theta 2}$. By contrast, the aerodynamic influence in terms of the ratio $C_L/C_{L\alpha}$ is rather small, though $C_{L\alpha}$ shows a significant decrease for hypersonic vehicles.

It is further shown that there is an upper limit of $T_{\theta 2}$. This limit is due to the atmospheric density gradient, which exerts a significant effect on aircraft dynamics in super- and hypersonic flight. The density gradient also yields a more rapid increase of $T_{\theta 2}$ when approaching its limit. As a result of general nature, the limit of $T_{\theta 2}$ is rather constant (in the order of 25–30 s), with practically no effect of Mach number and little influence of altitude.

References

1. "Flying Qualities of Piloted Aircraft," MIL-STD-1797, Jan. 1990.
2. "Flying Qualities of Piloted Airplanes," MIL-F-8785C, Sept. 1991.
3. Cox, T. H., and Jackson, D. W., "Evaluation of High-Speed Civil Transport Handling Qualities Criteria with Supersonic Flight Data," NASA TM 4791, April 1997.
4. Myers, T. T., Klyde, D. H., McRuer, D. T., and Suchomel, C., "Influence of Path-Attitude Lag in Hypersonic Flying Qualities," AIAA Paper 95-0555, Jan. 1995.

⁵Thompson, P. M., Myers, T. T., and Suhomel, C., "Conventional Autopilot Design for a Hypersonic Vehicle," AIAA Paper 95-0556, Jan. 1995.

⁶Larson, G. L., Klyde, D. H., Myers, T. T., and McRuer, D. T., "Military Missions and Linearized Model for a Hypersonic Vehicle," AIAA Paper 95-0851, Jan. 1995.

⁷Vu, P. T., and Biezad, D. J., "Direct-Lift Design Strategy for Longitudinal Control of Hypersonic Aircraft," *Journal of Guidance, Control, and Dynamics*, Vol. 17, No. 6, 1994, pp. 1260-1266.

⁸Schmidt, D. K., and Velapoldi, J., "Optimum Mission Performance and Guidance for Hypersonic Single Stage to Orbit," AIAA Paper 96-3904, July 1996.

⁹Schmidt, D. K., "Optimum Mission Performance and Multivariable Flight Guidance for Airbreathing Launch Vehicles," *Journal of Guidance, Control, and Dynamics*, Vol. 20, No. 6, 1997, pp. 1157-1164.

¹⁰Sachs, G., Schoder, W., and Kraus, W., "Separation of Lifting Vehicles at Hypersonic Speed—Wind Tunnel Tests and Flight Dynamics Simulation," *Space Systems Design and Development Testing*, AGARD CP 561, 1995, pp. 5-1-5-8.

¹¹Bowers, A., Noffz, G., Gonda, M., and Iliff, K., "A Generic Hypersonic Aerodynamic Model Example (GHAME)," NASA Dryden Flight Research Center, Edwards AFB, CA, 1989.

¹²Meyer, I., McMaster, I., and Moody, R., "Handling Qualities of the SR-71," Lockheed Aircraft Corp., Rept. SP-508, Advanced Development Projects, Burbank, CA, Sept. 1978.

¹³Heffley, R., and Jewell, W., "Aircraft Handling Qualities Data," NASA CR 2144, Dec. 1972.

¹⁴Sachs, G., "Path-Attitude Decoupling and Flying Qualities Implications in Hypersonic Flight," *Aerospace Science and Technology*, Vol. 2, No. 1, 1998, pp. 49-59.

Design Methods for Rocket Attitude Control Systems Subject to Actuator Saturation

Hyung Don Choi,* Hyochoong Bang,†
and Zeen Chul Kim‡

Korea Aerospace Research Institute,
Daejeon 305-600, Republic of Korea

Introduction

THE KSR Korea sounding rocket (KSR-II) is a two-stage sounding rocket with a payload capacity of about 150 kg. It is launched near vertically up to the altitudes in the 150-km range to carry out upper atmospheric experiments including ozone layer, ionospheric, and celestial x-ray measurement. A guidance and control (G&C) system is onboard to minimize the dispersion radius of the impact point. This system keeps the flight experiments less sensitive to meteorological conditions, wind in particular, by reducing the impact dispersion considerably. The attitude and angular velocities of the rocket necessary for the construction of the G&C system are obtained from an inertial navigation system (INS). Furthermore, a pneumatic S-19 (Ref. 1) actuator is adopted as a primary actuator system. The actuator saturation of the S-19 is a main element, which may degrade the performance of the whole system. For a controller with an integrator, the saturation effect is accumulated in the integrator, which increases the overshoot resulting in a high settling time.² This phenomenon is known as windup²⁻⁵ and usually results in performance degradation.

Received April 13, 1998; revision received Aug. 19, 1998; accepted for publication Aug. 20, 1998. Copyright © 1998 by the American Institute of Aeronautics and Astronautics, Inc. All rights reserved.

*Senior Research Scientist, Sounding Rocket Group, P.O. Box 113, Yuseung-Gu.

†Research Scientist, Koreasat Group, P.O. Box 113, Yuseung-Gu. Member AIAA.

‡Senior Research Scientist, Head of Satellite Bus Department, P.O. Box 113, Yuseung-Gu.

The primary goal of this Note is to apply the antiwindup controller (AWC) to KSR-II attitude control. There have been extensive studies with well-developed theories on AWC, including stability analysis.²⁻⁵ A rather simple form of AWC, however, is applied to the practical problem of launch vehicle control in this study. The control design is viewed from application perspectives instead of conducting theoretical development. A modified AWC also is introduced, which compensates the highly gain-sensitive characteristics of the typical AWC.

Description of KSR-II Control System

The control system of the KSR-II consists of an INS, a controller, the S-19, and rocket aerodynamics. Because the shape of the KSR-II is long and slender, the magnitude of the roll moment of inertia is approximately 1/100 of the pitch and yaw moments. The roll angular velocity caused by thrust and fin misalignment is much greater than the pitch and yaw angular counterparts. Thus, an INS with a roll-isolated inertial measurement unit by a gimbal is selected. The INS calculates the pitch and yaw angle by a strap-down technique and measures the roll angle. The KSR-II controls attitude by producing aerodynamic control moments using canard fins actuated by a pneumatic system. This S-19 pneumatic system is designed to accept control inputs in the form of roll-resolved pitch and yaw commands to two pneumatic servos. There are four canards connected in pairs with one pair controlling each lateral axis. S-19 has maximum actuating limits at 22 deg in deflection and 140 deg/s in slew rate. This actuator saturation affects the control system performance and stability significantly. The attitude of KSR-II is controlled by canard fins up to 20 s after launch, corresponding to the thrusting phase of the first and second stages. At the end of the control time, the altitude reaches 9.2 km and the Mach number is 3.0. The maximum value of the rocket natural frequency is about 2 Hz, and the damping coefficient is about 0.06 during the first stage burning and 0.002-0.04 for the second stage. The maximum axial accelerations are 12 and 9 g for the first and second stages, respectively. The dynamic pressure reaches a maximum value at about 22 s after launch.

AWC

To maintain the initial rocket attitude at liftoff for a certain period of time, the following proportional, integral, plus derivative (PID) compensator is designed as

$$\delta_p = k \left(e_p + \frac{1}{T_i} \int e_p dt + T_d \dot{e}_p \right) \quad (1)$$

where $e_p = \theta_c - \theta$ is pitch error, θ_c is pitch command, θ is actual pitch angle, k is controller gain, T_i and T_d are integral and derivative time constants, and δ_p is the compensator output. In this study, $k = 10$, $T_i = 3$ s, and $T_d = 0.3$ s are used, which result in gain margins of 10 and 7.6 dB, phase margins of 43.2 and 34.2 deg, and bandwidths of 28 and 43 rad/s for the first and second stage controls, respectively. For a controller with an integrator, the effect of the actuator saturation is accumulated in the integrator, and the integrator value becomes excessively large, i.e., windup. A partial solution for the windup problem of the KSR-II is sought by applying a typical AWC design technique. Because the limit of deflection angle is more severe than that of slew rate in the S-19, only the actuating limit of deflection angle is considered. The concept of AWC is to reduce the difference between the compensator output and the actuator control input by feeding back the difference caused by the actuator limit. The feedback signals of the difference, as well as the PID compensator, are combined together in the AWC as

$$\delta_p^w = k \left(e_p + \frac{1}{T_i} \int e_p dt + T_d \dot{e}_p \right) - \int f dt \quad (2)$$

where the new error term is defined as

$$f = (k/T_i)(\delta_p^w - u_p^w) \quad (3)$$